JOC*Note*

Kinetic Studies on the Thermal *cis*-to-*trans* Isomerization of 1-Phenyltriazenes Derived from Cyclic Amines

Jinlong Fu, Kelvin Lau, and Mónica Barra*

Department of Chemistry, University of Waterloo, Waterloo, Ontario, Canada N2L 3G1

mbarra@uwaterloo.ca

Received October 28, 2008

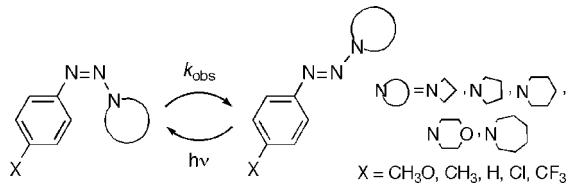

Rate constants for thermal *cis*-to-*trans* isomerization of *N*-(phenylazo)-substituted nitrogen ring heterocyles were determined as a function of phenyl ring substitution, cyclic amine ring size, and organic solvents. Observed first-order rate constants are found to increase with increasing electron-withdrawing character of the *para* substituent, with larger amine rings, and with increasing solvent polarity. Overall, trends observed are consistent with geometrical isomerization taking place through rotation around the nitrogen−nitrogen double bond via a polarized transition state.

Reversible *cis*−*trans* (*Z*−*E*) isomerizations, induced at least in one direction by absorption of light, represent one of the most common chemical processes involved in photochromic materials.[1] *Z*−*E* photoisomerable compounds have been shown to present many interesting features not only of fundamental importance but also of utility in various applications and fields ranging from sensors to molecular devices to biomedicine.[2]

An interesting class of photochromic material based on *cis*−*trans* isomerization around a nitrogen−nitrogen double bond is represented by triazenes, compounds characterized by having a diazoamino group (−N(1)═N(2)−N(3)<) and of potential utility in photoresponsive materials. A thorough understanding of the isomerization mechanism(s) involved in triazene systems is certainly vital to control and exploit this class of photochromic material. However, there are only a handful of mechanistic studies on the *cis*−*trans* isomerization of triazenes,[3−5] and these are based on 1,3-diphenyltriazenes, substrates for which thermal *cis*-to-*trans* isomerization is shown to involve 1,3-prototropic rearrangements.[4,5] Trisubstituted triazenes, on the other hand, may undergo thermal *cis*-to-*trans* isomerization by way of (a) a rotation mechanism (i.e., via a transition state involving heterolytic rupture of the −N═N− π-bond) or (b) an inversion mechanism (i.e., via a transition state involving a linear sp hybridized nitrogen), similarly to the case of azobenzenes.[6]

CHART 1. Target Substrates

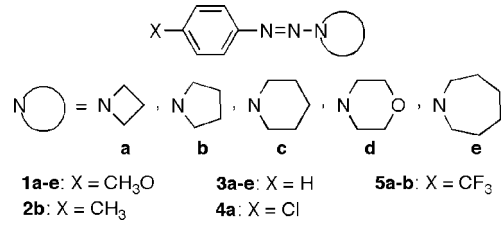

The work presented here focuses on the thermal *cis*-to-*trans* isomerization of a series of 1-phenyltriazenes derived from cyclic amines (Chart 1). Rate constants for isomerization were measured to assess the effects of varying the phenyl ring substituent, cyclic amine ring size, and solvent polarity. A comparison with data obtained by means of computational simulations is also presented.

cis-Triazenes were generated upon irradiation (at 350 nm) of corresponding *trans* isomers dissolved in various organic solvents. In all cases, *trans*-to-*cis* photoisomerization leads to a decrease in absorbance around λ_{max} of the longer wavelength band, since *cis* isomers typically have lower absorptivity than *trans* forms in this spectral region.[3−5] With a few exceptions (systems for which photolytic decomposition is significant; see below) the initial absorbance, however, is re-established in the dark as the *cis* forms spontaneously isomerize back to the *trans* isomers. Corresponding recovery (growth) traces follow first-order kinetics (Figure 1 is representative), and resulting observed rate constants are summarized in Tables 1 and 2.[7]

Comparison of k_{obs} values for compounds **1a**−**e** (Table 1) and **3a**−**e** (Table 2) clearly indicates an increase in reactivity with increasing ring size as well as with decreasing electronegativity of the ring atoms, i.e., **d** versus **c**, regardless of the solvent. In regards to the effect of phenyl ring substitution, comparison of values for compounds **1a** and **3**−**5a**, as well as for compounds **1**−**3b** and **5b**, shows an increase in reactivity with increasing electron-withdrawing character. Lastly, for any given substrate an increase in reactivity is typically observed with increasing solvent polarity. Interestingly, the more electron-withdrawing the phenyl substituent and the larger the cyclic amino moiety, the more significant the solvent effect is.

(1) *Photochromism: Molecules and Systems*; Dürr, H., Bouas-Laurent, H., Eds.; Elsevier: Amsterdam, 1990.
(2) Dugave, C.; Demange, L. *Chem. Rev.* **2003**, *103*, 2475.
(3) Baro, J.; Dudek, D.; Luther, K.; Troe, J. *Ber. Bunsen-Ges. Phys. Chem.* **1983**, *87*, 1155.
(4) Scaiano, J. C.; Chen, C.; McGarry, P. F. *J. Photochem. Photobiol., A* **1991**, *62*, 75.
(5) (a) Barra, M.; Chen, N. *J. Org. Chem.* **2000**, *65*, 5739. (b) Chen, N.; Barra, M.; Lee, I.; Chahal, N. *J. Org. Chem.* **2002**, *67*, 2271. (c) Zhang, H.; Barra, M. *J. Phys. Org. Chem.* **2005**, *18*, 498.
(6) Knoll, H. In *CRC Handbook of Organic Photochemistry and Photobiology*; Horspool, W. M., Lenci, F., Eds.; CRC Press: Boca Raton, 2004, 89/1, and references therein.
(7) The largest first-order rate constant that can be determined with our system is ca. 0.15 s^{-1}.

10.1021/jo8024048 CCC: $40.75
Published on Web 01/09/2009

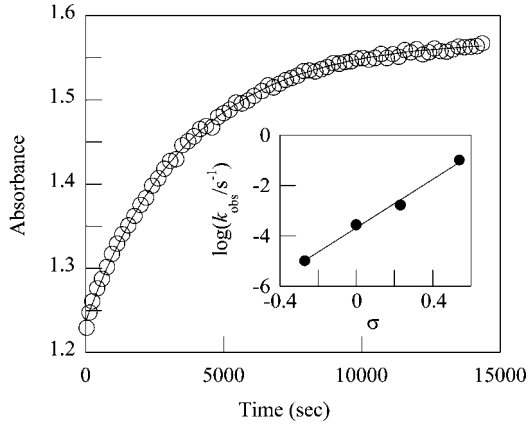

FIGURE 1. Kinetic trace recorded at 325 nm for *cis*-to-*trans* isomerization of **3a** in MeCN solution. Inset: Hammett dependence of the first-order rate constants for thermal *cis*-to-*trans* isomerization of compounds **1a** and **3**−**5a** in MeCN solution.

TABLE 1. Observed Rate Constants for Isomerization of Compound 1

	k_{obs} (10^{-2} s^{-1})[a]				
solvent[b]	**1a**	**1b**	**1c**	**1d**	**1e**
c-HexH	*c*	*c*	*c*	*c*	3.19 (5)
PhH	*c*	0.16 (1)	1.92 (4)	*c*	7.8 (4)
MeCN	0.00102 (4)	0.35 (2)	7.1 (1)	0.49 (2)	>15
DMF	0.000524 (8)	0.30 (1)	7.3 (1)	0.652 (8)	>15
DMSO	0.0041 (3)	0.49 (2)	13.2 (4)	1.47 (4)	>15

[a] Error for last significant figure given in brackets; T = 21 °C. [b] In solvents other than MeCN, solutions contain 1.3% MeCN. Alcohols were excluded as solvents due to considerable photolytic decomposition. [c] Photolytic decomposition >10%.

TABLE 2. Observed Rate Constants for Isomerization of Compounds 2−5

	k_{obs} (10^{-2} s^{-1})[a]					
solvent[b]	**2b**	**3a**	**3b**	**3d**[c]	**4a**	**5a**[c]
c-HexH	0.23 (2)	*d*	0.59 (2)	2.62[e] (8)	0.027 (5)	0.224 (3)
PhH	0.47 (1)	0.0032 (1)	2.54 (3)	7.2 (2)	0.0130 (3)	0.98 (2)
MeCN	2.45 (7)	0.0279 (8)	12 (2)	>15	0.166 (6)	10.3 (5)
DMF	2.70 (8)	0.0314 (5)	14 (3)	>15	0.239 (4)	<15
DMSO	4.3 (1)	0.0611 (1)	>15	>15	0.396 (8)	<15
MeOH	2.8 (2)	0.0258 (8)	3.52 (7)	<15	0.072 (2)	4.00 (8)
2-PrOH	0.30 (1)	0.0044 (2)	1.58 (3)	4.5 (2)	0.0232 (3)	1.88 (1)
1-BuOH	0.34 (1)	0.0070 (3)	1.62 (3)	4.2 (1)		1.75 (1)
1-OctOH	*d*	0.0100 (2)	1.80 (6)	6.6 (4)	0.0223 (1)	1.67 (2)

[a] Error for last significant figure given in brackets; T = 21 °C. [b] In solvents other than MeCN, solutions contain 1.3% MeCN. [c] Rate constants for **3e** (in *c*-HexH or MeCN) and **5b** (in *c*-HexH, MeCN or MeOH) are too fast to be measured with our system. [d] Photolytic decomposition >10%. [e] Value for **3c** = 0.104 (8) s^{-1}; in any other solvent, k_{obs} > 0.15 s^{-1} for **3c**.

The trends referred to above can be interpreted in terms of an internal rotation mechanism involving twisting around the C−N═N−N dihedral angle via heterolytic rupture of the N(1)═N(2) π-bond, as illustrated in Scheme 1. This pathway is analogous to the rotational mechanism characteristic of donor/acceptor-substituted ("push−pull") azobenzenes.[6]

The energy barrier for the polar mechanism illustrated in Scheme 1 will be influenced by the ability of the phenyl ring and the cyclic amino moiety to stabilize, respectively, the negative and positive charges in the polarized transition state. Moreover, these two functional groups will also greatly affect the contributions of the 1,3-dipolar resonance form **B** (eq 1)

SCHEME 1

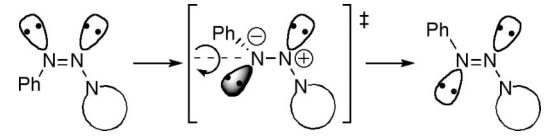

characteristic of triazenes and key in determining the N(1)═N(2) bond order of the ground state *cis*-structure and, hence, the rotational energy barrier.[8]

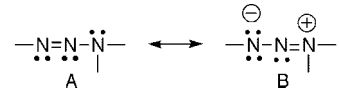

(1)

The electron-donating character of N(3) for the triazene series studied, and therefore the ability of N(3) to stabilize a positive charge will depend on the size of the cyclic amino moiety. For cyclic amines, the intrinsic electron-donating ability of N (ρ_{oc}, evaluated by the reactive hybrid orbital theory)[9] and ionization potential (IP) values[10] are shown to decrease and increase, respectively, with decreasing ring size (e.g., ρ_{oc} = 2.333, 2.365, 2.372 and IP = 9.04, 8.77, 8.64 eV for azetidine, pyrroline, and piperidine, respectively). These trends can be rationalized in terms of the change in hybridization of the nitrogen atom, i.e., as the ring size decreases the s-character of the nitrogen lone pair orbital increases, which in turn implies the lone pair electrons are held more tightly by N. Thus, the increase in rate constants for thermal *cis*-to-*trans* isomerization observed experimentally as the amine ring size increases along the triazene series from **a** to **e** is consistent with an increase in the electron-donating character of N(3),[11] which leads to a decrease in the N(1)═N(2) bond order (by increasing the contribution of the 1,3-dipolar canonical form **B** to the ground state *cis*-structure) as well as to an increase in the stability of the polar transition state. In addition, the noticeable decrease in reactivity in the case of morpholine (**d**) derivatives relative to that of piperidine (**c**) is attributed to the lower availability of the N(3) lone pair electrons due to the inductive (−I) effect of oxygen.

The increase in reactivity with increasing electron-withdrawing character of the phenyl ring substituent is rationalized in terms of its influence on the ability of N(1) to stabilize a negative charge, i.e., as the electron-withdrawing character of the *para* substituent increases, the stability of a negative charge on N(1) increases, thus leading to a decrease in the N(1)═N(2) bond order in the ground state *cis*-structure, as well as to an increase in the stability of the polar transition state and, hence, to a decrease in the energy barrier for (rotational) isomerization. A Hammett plot for rate constants corresponding to compounds **1a** and **3**−**5a** in MeCN solutions (Figure 1, inset) renders a Hammett reaction constant (ρ) value of (4.8 ± 0.3).[12] This (relatively) large positive ρ value is fully consistent with an increase in electron density at N(1) as rotation around the N(1)═N(2) bond takes place.

(8) (a) Barra, M.; Srivastava, S.; Brockman, E. *J. Phys. Org. Chem.* **2004**, *17*, 1057. (b) Barra, M.; Lim, H. *Trends Org. Chem.* **2006**, *11*, 17.

(9) Ohwada, T.; Hirao, H.; Ogawa, A. *J. Org. Chem.* **2004**, *69*, 7486.

(10) Yoshikawa, K.; Hashimoto, M.; Morishima, I. *J. Am. Chem. Soc.* **1974**, *96*, 288.

(11) Plots of log(k_{obs}), for data corresponding to **1a**−**c** (MeCN, DMF, or DMSO) against ρ_{oc} or IP (for azetidine, pyrrolidine, and piperidine) show very good linear correlations.

(12) Unfortunately, Hammett reaction constants for other solvent(s) or types of substrate (i.e., ring size) could not be determined since there is insufficient data for a significant correlation.

TABLE 3. Selected Geometric Parameters and Rotational Barriers Calculated at the B3LYP/6-31G* Level in the Gas Phase

	cis-compound[a]													
parameter	**1a**	**1b**	**1c**	**1d**	**1e**	**2b**	**3a**	**3b**	**3c**	**3d**	**3e**	**4a**	**5a**	**5b**
N(1)═N(2)[b]	1.257	1.257	1.252	1.250	1.258	1.257	1.257	1.257	1.253	1.251	1.258	1.258	1.259	1.259
	(1.265)	(1.271)	(1.266)	(1.260)	(1.267)	(1.272)	(1.266)	(1.272)	(1.266)	(1.263)	(1.268)	(1.272)	(1.274)	(1.278)
N(2)−N(3)[b]	1.365	1.372	1.401	1.407	1.370	1.365	1.357	1.363	1.382	1.388	1.362	1.354	1.349	1.355
	(1.323)	(1.321)	(1.332)	(1.338)	(1.328)	(1.318)	(1.319)	(1.318)	(1.329)	(1.333)	(1.325)	(1.311)	(1.306)	(1.308)
C−N═N−N[c]	−7.6	11.1	8.3	8.0	−10.6	11.5	7.7	11.9	8.9	8.4	−11.0	8.1	8.5	13.5
	(−89.5)	(91.6)	(89.4)	(89.3)	(−89.0)	(91.7)	(89.4)	(91.5)	(89.1)	(89.3)	(−88.8)	(89.2)	(89.1)	(91.2)
dipole[d]	3.716	3.557	3.339	2.950	3.909	3.788	3.792	3.812	3.510	2.277	3.424	3.872	4.427	4.893
	(5.030)	(5.405)	(4.877)	(3.062)	(4.882)	(5.886)	(5.644)	(6.064)	(5.710)	(3.892)	(5.528)	(7.901)	(9.066)	(9.413)
ΔE[e]	24.9	20.9	19.2	20.1	19.0	19.3	22.5	18.6	16.7	17.6	16.3	21.8	19.8	16.0

[a] Transition state (TS) values given in brackets. [b] Angstroms. [c] Degrees. [d] Debye. [e] ($E_{TS} - E_{cis}$) in kcal/mol; ZPE correction included.

In regards to the solvent effects, the fact that observed rate constants for thermal *cis*-to-*trans* isomerization increase with increasing solvent polarity suggests an increase in molecular dipole moment on going from ground state (*cis*) to transition state, as illustrated by the polar mechanism given in Scheme 1. The effects of solvent on substrate photolytic decomposition should be mentioned here as well. It is well-known that triazenes can decompose upon UV irradiation via N(2)−N(3) bond fission.[13] In fact, triazenes can be effectively used as photolabile compounds in polymers designed for laser microstructuring (laser ablation lithography).[14] Rate constants given in Tables 1 and 2 correspond to systems for which substrate photolytic decomposition (if at all significant) is well below 10% (typically <1%). However, for compounds **1a**−**d** (i.e., substrates containing the strongest electron-donating phenyl substituent studied) percent decompositions in alcohol solutions systematically exceed 20% (see Supporting Information). This significant substrate decomposition is thought to result from a decrease in the double bond character of the N(2)−N(3) bond by stabilization of the canonical form **A** (eq 1) through hydrogen bonding of the N(3) lone pair electrons with the hydrogen bond donor solvent.[15] Not surprisingly, decomposition of compounds **1a**−**d** is significant as well in cyclohexane (poorest solvent, among those employed, for stabilization of charge-separated structures). Overall, photolytic decomposition is found to be of importance under conditions where stabilization of the dipolar form **B** (eq 1) is indeed quite unfavorable. In fact, increased photolytic decomposition of 1-aryltriazenes bearing electron-donating (or poor electron-withdrawing) phenyl ring substituents in protic (vs aprotic) polar media and apolar (vs polar) media is not unprecedented.[16] In addition to significant photolytic decomposition, compounds **1a**−**d** in alcohol or cyclohexane solutions typically yielded traces that followed complex kinetics (tentatively attributed to the involvement of a radical decomposition mechanism);[13,16] these systems, however, were not studied in any further detail.

Thermal *cis*-to-*trans* isomerization of target substrates was investigated as well by means of theoretical calculations. Optimized conformations of target triazenes and potential energy curves for isomerization in the gas phase were determined by using ab initio methods. Table 3 summarizes (selected) optimized geometric parameters for *cis* triazenes and corresponding transition states (located using the QST2 option), together with calculated energy barriers for *cis*-to-*trans* isomerization. In all cases, the transition state obtained shows, in comparison to the ground-state *cis* structure, (i) lengthening of the N(1)═N(2) bond, (ii) shortening of the N(2)−N(3) bond, (iii) increased C−N═N−N dihedral angle, and (iv) larger molecular dipole moment. These results clearly support the rotation mechanism depicted in Scheme 1. Moreover, calculated energy barriers for *cis*-to-*trans* isomerization (ΔE, Table 3) follow the same trends as those inferred from comparison of the rate constants experimentally observed, i.e., reactivity increases with increasing electron-withdrawing character of the phenyl ring substituent and with increasing cyclic amine ring size. Also, potential energy curves for isomerization of **3b** (Figure S1, Supporting Information) show that the energy barrier for the rotation mechanism is lower than that for the inversion pathway. Interestingly, this result (i.e., rotation more favorable than inversion) contrasts with those from a recent work on thermal isomerization of azocompounds, which shows that for azobenzene (AB) the energy barrier for CNN inversion is lower than that for CNNC rotation, whereas for *p*-amino-azobenzene (AAB) the energy barriers along both the rotation and inversion pathways are quite similar.[17] In fact, the lower rotational energy barrier for *cis*-to-*trans* isomerization of **3b** (ca. 19 kcal/mol) relative to that of AAB (ca. 24 kcal/mol) and AB (ca. 33 kcal/mol) would reflect the importance of the 1,3-dipolar resonance form **B** (eq 1) in determining the properties of diazoamino compounds.

In summary, the present study shows that the rate of return from *cis* to *trans* for 1-phenyltriazenes derived from cyclic amines increases, in organic solvents, as the electron-withdrawing character of the phenyl ring substituent, the cyclic amine ring size, and the polarity of the solvent increase as well. All of the presented data (in particular, the large influence of the nature of the cyclic amino moiety) are in accord with an internal rotation mechanism, in which stabilization of charge-separated structures is crucial.

Experimental Section

Synthesis of Triazenes. Triazenes were synthesized, under mildly basic conditions, by means of aniline-diazonium salts coupling via the classical diazotization method with $NaNO_2$, according to literature procedures.[18,19] Crude products were purified by recrystallization from petroleum ether (unless stated otherwise).

(13) Lippert, T.; Stebani, J.; Nuyken, O.; Stasko, A.; Wokaun, A. *J. Photochem. Photobiol., A* **1994**, *78*, 139.
(14) Lippert, T.; Dickinson, J. T. *Chem. Rev.* **2003**, *103*, 453.
(15) Anet, F. A. L.; Ji, X. *Tetrahedron Lett.* **1984**, *25*, 1419.
(16) Panitz, J. C.; Lippert, T.; Stebani, J.; Nuyken, O.; Wokaun, A. *J. Phys. Chem.* **1993**, *97*, 5246.
(17) Wang, L.; Wang, X. *J. Mol. Struct. (Theochem)* **2007**, *806*, 179.
(18) Foster, N. I.; Heindel, N. D.; Burns, H. D.; Muhr, W. *Synthesis* **1980**, *7*, 572.
(19) Ludwig, M.; Bednářová, I.; Pařík, P. *Collect. Czech. Chem. Commun.* **1999**, *64*, 1654.

Melting points and ^{1}H NMR data for known triazenes (see Supporting Information) are all in excellent agreement with reported values.

***N*-(4-Methoxyphenylazo)azetidine (1a).** Dark brown crystals; mp 48−49 °C; ^{1}H NMR (300 MHz, $CDCl_3$) δ 7.40−7.37, 6.87−6.84 (AA′XX′, 4H), 4.24 (app. t, J = 7.5 Hz, 4H), 3.79 (s, 3H), 2.33 (app quintet, J = 7.5 Hz, 2H); ^{13}C NMR (500 MHz, DMSO-d_6) δ 157.8, 143.6, 121.4, 114.1, 55.2, 54.8, 15.3; IR (CH_2Cl_2) 2978, 2883, 1605, 1585, 1503, 1442, 1409, 837 cm^{-1}; MS *m*/*z* (rel intensity) (EI) 191 [M, 46], 135 (60), 107 (100), 92 (35), 77 (45); HRMS calcd for $C_{10}H_{13}N_3O$ 191.1059, found 191.1055.

***N*-(4-Methoxyphenylazo)perhydroazepine (1e).** Light brown solid; mp 45−46 °C; ^{1}H NMR (300 MHz, $CDCl_3$) δ 7.35−7.33, 6.86−6.83 (AA′XX′, 4H), 4.00−3.68 (br and s overlapped, 7H), 1.80 (br, 4H), 1.59 (br, 4H); ^{13}C NMR (500 MHz, $CDCl_3$) δ 157.3, 145.3, 121.2, 114.0, 55.4, 28.7; IR (CH_2Cl_2) 2933, 2856, 1604, 1584, 1503, 1460, 1408, 834 cm^{-1}; MS *m*/*z* (rel intensity) (EI) 233 [M, 51], 135 (46), 107 (100), 92 (16), 77 (23); HRMS calcd for $C_{13}H_{19}N_3O$ 233.1528, found 233.1530.

***N*-(Phenylazo)azetidine (3a).** Product was isolated from reaction medium by solvent extraction (with diethyl ether) to afford a yellow oil; ^{1}H NMR (300 MHz, acetone-d_6) δ 7.36 (d, J = 7.4 Hz, 2H), 7.30 (t, J = 7.4 Hz, 2H), 7.14 (t, J = 7.4 Hz, 1H), 4.24 (app t, J = 7.1 Hz, 4H), 2.36 (app quintet, J = 7.5 Hz, 2H); ^{13}C NMR (500 MHz, $CDCl_3$) δ 150.4, 128.9, 126.3, 120.7, 55.0, 15.8; IR (CH_2Cl_2) 2973, 2882, 1596, 1585, 1483, 1459, 766 cm^{-1}; MS *m*/*z* (rel intensity) (EI): 161 [M, 37], 105 (48), 77 (100); HRMS calcd for $C_9H_{11}N_3$ 161.0953, found 161.0949.

***N*-(4-Chlorophenylazo)azetidine (4a).** Crude product was purified by recrystallization from ethanol to afford a light brown solid; mp 56−57 °C; ^{1}H NMR (300 MHz, acetone-d_6) δ 7.38−7.29 (AA′BB′, 4H), 4.27 (br, 4H), 2.38 (app quintet, J = 7.5 Hz, 2H); ^{13}C NMR (500 MHz, $CDCl_3$) δ 149.0, 131.4, 128.9, 121.8, 55.2, 15.8; IR (CH_2Cl_2) 2978, 2884, 1484, 1396, 835 cm^{-1}; MS *m*/*z* (rel intensity) (EI) 195 [M (^{35}Cl), 26], 139 (44), 113 (32), 111 (100); HRMS calcd for $C_9H_{10}{}^{35}ClN_3$ 195.0563, found 195.0564.

***N*-(4-Trifluoromethtylphenylazo)azetidine (5a).** Yellow crystals; mp 78−80 °C; ^{1}H NMR (300 MHz, $CDCl_3$) δ 7.57−7.54, 7.49−7.46 (AA′BB′, 4H), 4.37 (app t, J = 7.3 Hz, 4H), 2.41 (app quintet, J = 7.6 Hz, 2H); ^{13}C NMR (500 MHz, $CDCl_3$) δ 153.1, 127.5 (q, $^2J_{C-F}$ = 32.3 Hz), 126.0 (q, $^3J_{C-F}$ = 3.8 Hz), 124.4 (q, $^1J_{C-F}$ = 272 Hz), 120.6, 55.3, 15.7; IR (CH_2Cl_2) 2887, 1612, 1399, 1322, 848 cm^{-1}; MS *m*/*z* (rel intensity) (EI) 229 [M, 19], 173 (29), 145 (100); HRMS calcd for $C_{10}H_{10}F_3N_3$ 229.0827, found 229.0824.

***N*-(4-Trifluoromethylphenylazo)pyrrolidine (5b).** Bright orange flakes; mp 113−114 °C; ^{1}H NMR (300 MHz, $CDCl_3$) δ 7.55−7.52, 7.46−7.44 (AA′BB′, 4H), 3.92 (br, 2H), 3.67 (br, 2H), 2.03 (m, 4H); ^{13}C NMR (500 MHz, acetone-d_6) δ 155.5, 126.8 (q, $^3J_{C-F}$ = 3.8 Hz), 126.4 (q, $^2J_{C-F}$ = 31.1 Hz), 125.7 (q, $^1J_{C-F}$ = 271 Hz), 121.2, 51.8, 47.2, 24.4, 24.0; IR (CH_2Cl_2) 2879, 1612, 1402, 1316, 848 cm^{-1}; MS *m*/*z* (rel intensity) (EI) 243 [M, 20], 173 (27), 145 (100); HRMS calcd for $C_{11}H_{12}F_3N_3$ 243.0983, found 243.0983.

Methods. Solvents (OmniSolv grade, except for 1-BuOH and 1-OcOH, ACS grade) were used as received. Solutions of triazenes (having an absorbance of ca. 0.5 at 350 nm when placed in quartz cells constructed of 7 × 7 mm Suprasil tubing) were prepared by transferring 64 μL of an appropriate stock triazene solution in acetonitrile to a 5-mL flask and diluting to the mark with desired organic solvent; 2-mL aliquots were subsequently placed in 7 × 7 mm quartz cells. Samples were irradiated using a Rayonet photoreactor fitted with one RPR-3500 Å lamp. After an irradiation period of 30 s, samples were quickly transferred to a spectrophotometer (equipped with a thermotasted cell compartment connected to a circulating water bath) where kinetic traces corresponding to *cis*-to-*trans* isomerization were recorded by measuring the increase in absorbance (at 325 nm) as a function of time. All measurements were carried out at (21.0 ± 0.1) °C using air-equilibrated samples. Values for the observed rate constants were obtained by fitting the kinetic traces to a single exponential function. Reported values correspond to the average of two to four independent runs. Percent decomposition values were determined by comparing the absorbance obtained at the end of the thermal growth with that recorded before irradiation. In no case did light exposure in the conventional spectrophotometer lead to any detectable photoisomerization or photodecomposition.

Calculations were performed using the Gaussian03 package of programs.[20] Full geometry optimization were performed using DFT-B3LYP method and 6-31G* basis set.

Acknowledgment. Financial support from the Natural Sciences and Engineering Research Council (NSERC) of Canada and the University of Waterloo is gratefully acknowledged.

Supporting Information Available: Full citation for ref 20, general synthesis procedure, analytical data for known compounds, copies of NMR spectra for new compounds, photolytic decomposition yields, UV−vis absorption spectra (MeCN solution) for all compounds (*trans* form), potential energy curves for rotation and inversion pathways for **3b**, and calculated geometries (coordinates), imaginary frequencies (where applicable), and energies of all stationary points. This material is available free of charge via the Internet at http://pubs.acs.org.

JO8024048

(20) Frisch, M. J. et al. *Gaussian 03, Revision C.02*; Gaussian, Inc.: Wallingford, CT, 2004.